JOURNAL OF MATERIALS SCIENCE: MATERIALS IN MEDICINE **16** (2005) 247–252

Cytocompatibility of novel tin oxide thin films

N. RUSHE[1,*], M. BALL[1], W. M. CARROLL[1], S. HEALY[2], J. MCMANUS[2], D. CUNNINGHAM[2]
[1]*National Centre for Biomedical Engineering Science, National University of Ireland, Galway, Ireland*
[2]*Inorganic Chemistry Department, National University of Ireland, Galway, Ireland*
E-mail: niamh.rushe@nuigalway.ie

The capacity of tin oxide films to support cell growth was investigated. Three substrates were used for the test: glass coverslips, glass coverslips spin coated with tin oxide and commercially available 316 stainless steel. The wettabilities and surface roughness of the three surfaces were measured before seeding 3T3 fibroblasts onto the samples. The behaviour of the cells grown on the tin oxide was compared to the uncoated glass and the steel and results showed that the cell growth on tin oxide compared favourably with the other substrates. The surface wettability appeared to have the strongest effect on cell adhesion to tin oxide.
© *2005 Springer Science + Business Media, Inc.*

1. Introduction

Thin films are already used on a variety of medical devices including orthopaedic implants [1–3], cardiovascular products [4, 5], surgical instruments [6], orthodontic and dental instruments [7, 8]. The fundamental value of coating technology rests in the ability to modify the surface properties of a device without changing the bulk properties and biomechanical/biomedical functionality.

Tin oxide films have a number of standard applications in the glass [9–12] and gas sensing industries [13, 14], but details on biological uses of these films are scarce in the literature. There are some references involving cell growth on indium tin oxide (ITO). One such example is from Lucas *et al.* [15]. This group established that indium tin oxide (ITO) has no toxic effects on cultured CNS cells. Cells grown on ITO were also used by another group [16] to examine gap junctional intercellular communication (GJIC) levels in human lung carcinoma cells, and again to improve the efficiency of labelling of adherent cells with radioactive ^{32}P [17]. It has also been shown that ITO thin film conductors can be used for repeated and long term electrical stimulation of monolayer networks in culture while still remaining functional as recording electrodes [18]. In all instances the tin oxide was commercially purchased and no details of the properties of the doped tin oxide film itself were discussed. Whilst tin containing films do not appear intrinsically toxic, there are no details of the effects of pure tin oxide films.

In this paper results from cytotoxicity tests on a tin oxide film deposited in a novel way will be described. Tin oxide films are usually deposited by CVD [19–22], PVD [14, 23, 24] or the sol-gel [25, 26] methods. In the present study the tin oxide films were deposited by the spin coating method from solution. This is the first example of the use of this soluble form of tin oxide and the synthesis will be described at a later stage. This paper presents the details of the potential of these tin oxide film for biomedical applications. 316 stainless steel is used for a number of biomedical applications, for example stents and information regarding cell reactions to that material is abundant in the literature. This was one of the substrates used in this study. Glass coverslips and glass coverslips coated with tin oxide were also used and the results from each substrate were compared.

A number of parameters were assessed on cells seeded onto the samples. These were Almar Blue, total DNA and cell spreading. The Almar Blue assay is designed to measure quantitatively the metabolic activity of various human and animal cell lines [27]. The Almar Blue assay incorporates a fluorometric/calorimetric growth indicator based on detection of metabolic activity. Specifically, the system incorporates an oxidation/reduction indicator that both fluoresces and changes colour in response to chemical reduction of growth medium resulting from cell growth.

Measurement of total DNA is a reliable measure of cell number. Determination of DNA with the fluorochrome bisbenzimidazole (Hoechst 33258) is well established [28]. This determination is based on the enhanced fluorescence and shift in the emission wavelength of the fluorochrome Hoechst 33258 upon binding cellular DNA. This results in a linear relationship

*Author to whom all correspondence should be addressed.

between fluorescence and DNA content over a broad range of DNA. This reaction is highly specific and other cellular components such as RNA, protein or carbohydrate do not cause significant fluorescence.

Cell spreading is a combined process of continuing adhesion and cytoplasmic contractile meshwork activity [29]. At first lamellar protrusions are formed. Microfilaments can always be observed in these lamellae. Focal adhesions are often associated with the tips of these protrusions. In a later stage, the ctyoplasmic flaps in between the protrusions also expand, completing cell spreading. The final analysis carried out on the seeded cells was to analysis the cell spreading. SEM images of the cells were collected and processed on Imagej software.

2. Materials & methods

2.1. Samples

Three different surfaces were used in this study. Glass coverslips from Esco (Erie Scientific Company, Portsmouth, N.H., USA), 316 stainless steel coupons supplied by Goodfellow, in Huntingdon in England. The tin oxide surface was prepared from a solution by the spin coating method onto the glass coverslips. The samples were spin coated at 3000 rpm, after which they were heated at 400 °C for twenty minutes. This coating procedure was repeated five times.

2.2. Contact angle

The contact angle of the stainless steel, glass and tin oxide surfaces was measured using the sessile drop method. An image of the drop was captured using a digital camera and the contact angle was measured using image analysis.

2.3. Surface roughness

The surface roughness of various samples was measured on the DI Dimension 3100 SPM system. The measurements were carried out on the stainless steel, glass and tin oxide surfaces in contact mode with a silicon nitride tip (Veeco). The roughness values used were Ra, the average roughness and Rms the root mean square roughness.

2.4. Cell growth

The samples were sterilised under UV light for 1 h, then rinsed with distilled water. 3T3 fibroblasts were maintained in cell culture incubator at 37 °C 5% CO_2 atmosphere in Dulbecco's modified Eagle's medium (DMEM, Sigma-Aldrich, Dublin, Ireland) supplemented with 10% (v/v) fetal calf serum and 1% penicillin/streptomycin. Freshly confluent flasks of 3T3's were incubated with trypsin for 5 min then resuspended in culture medium. Cells were counted using a hemacytometer and trypan blue and were seeded onto the surfaces at a density of 4×10^4cells cm^{-2}. Triplicate samples were used for each study. These were incubated in culture medium at 37 °C, 5% CO_2 for 24 h. Tissue culture media and reagents were obtained from Sigma.

2.5. Cell activity

The Almar Blue assay was used as a measure of cell metabolic activity. Cells were incubated on materials surfaces for appropriate time points. The culture medium was then removed and samples were washed with Hank's balanced salt solution to remove non-adherent cells. This was replaced with Almar Blue solution (Biosource) (1:9 dilution in Hank's balance salt solution). Samples were then incubated for 60 min at 37 °C. One hundred microlitre aliquots of this incubated solution were excited at 530 nm (excitation wavelength) and read at 590 nm (emission wavelength) using a Tecan Spectrafluorplus fluorimeter.

2.6. Scanning electron microscopy

Samples for SEM were fixed after specified intervals with 1.5% gluteraldehyde (Agar, UK) in 0.1 M sodium cacodylate buffer (Sigma) for 2 h and washed in 0.1 M sodium cacodylate buffer. Samples were dehydrated through a graded ethanol series, then dried via hexamethyldisilazane (Sigma). Samples were then gold coated and examined using a Hitachi S-4700 SEM with an accelerating voltage of 15 keV.

2.7. Total DNA

Total DNA was read by microfluorimetry. The media was removed from the cells and it was replaced with an equal amount of distilled water. The plates were frozen at −20 °C for 15 min then thawed at room temperature for 20 min. This was repeated three times. 100 μl aliquots of the resulting suspension were placed into a 96 well plate and diluted with 100 μl of a 20 μg/ml concentration of Hoechst 33258 in TNE buffer (10 mM Tris 1 mM ETDA and 2 M NaCl). A standard curve was constructed using calf thymus DNA, in TNE buffer. The plate was read at an excitation wavelength of 360 nm and an emission wavelength of 460 nm. A graph of concentration versus reading was plotted and the total DNA from the samples was calculated from this graph.

2.8. Circularity

The circularity of the cells was measured using Imagej software on images collected from the SEM. Firstly the samples were prepared for the SEM as described above. The image was then opened on the Imagej software and was thresholded. The cells were highlighted on the image and the circularity value was recorded. Circularity of 0 indicated an elongated polygon, whereas 1 was a perfect circle.

3. Results

3.1. Contact angle

The tin oxide had a contact angle of 12°, which means that it is hydrophilic, the glass had a contact angle of 43°

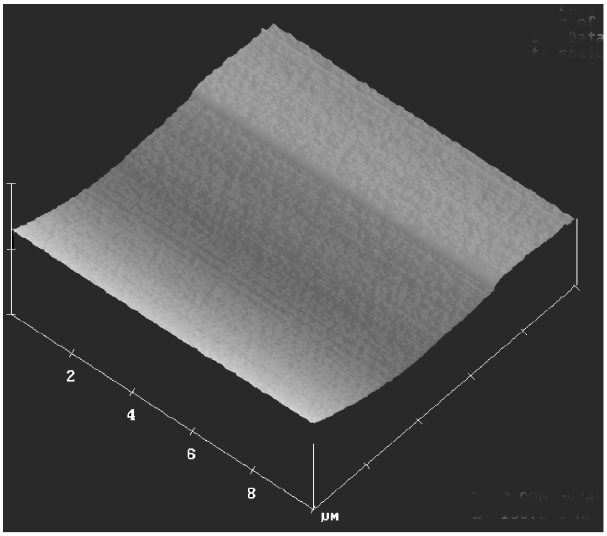

(a)

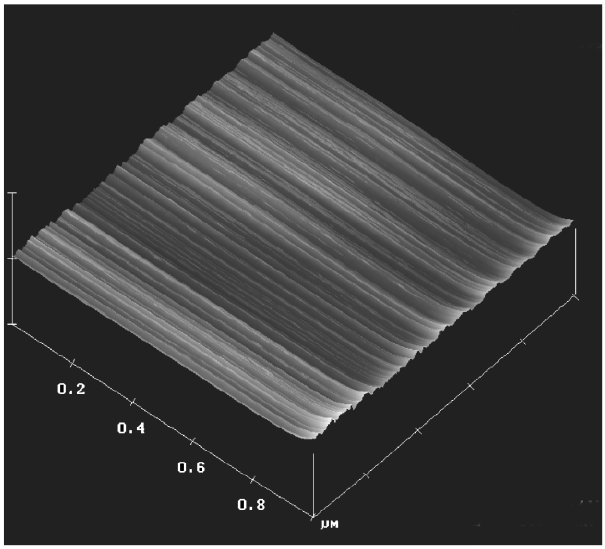

(b)

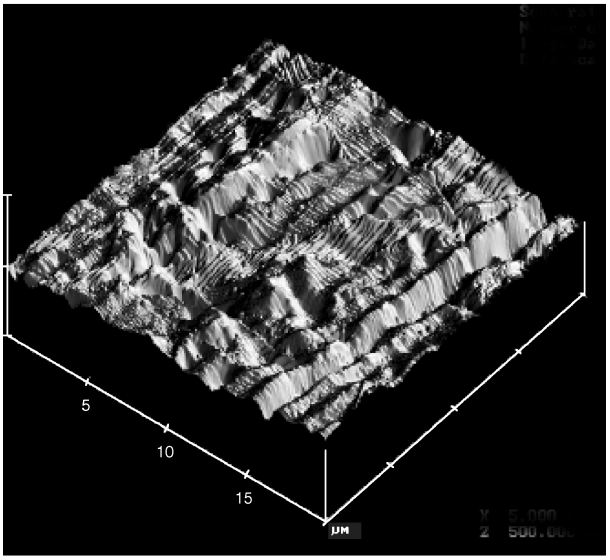

(c)

Figure 1 3 D AFM images of the substrates used in this study. (a) uncoated glass coverslip $R_a = 2.873$, $R_{ms} = 3.506$ (b) Tin oxide coated glass coverslip $R_a = 4.906$, $R_{ms} = 6.355$ (c) stainless steel sample $R_a = 39.591$, $R_{ms} = 52.480$.

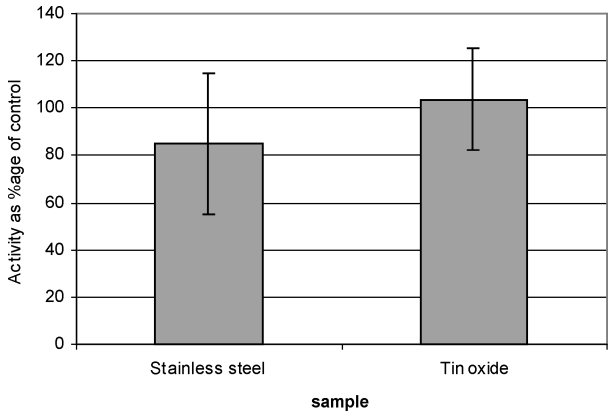

Figure 2 Graph of cell activity for cells grown on stainless steel and tin oxide coated glass as a percentage of the control (cells grown on glass). The statistical analysis shows that the results are not statistically different, i.e., the cells are as active on tin as on the other substrates (one way ANOVA, $p = 0.256$ and $f = 1.722$).

and the stainless steel had a contact angle of 57°, which makes the glass and steel substrates more hydrophobic than the tin oxide.

3.2. Surface roughness

The surface roughness of the coverslips and the tin oxide surfaces were low compared with the surface roughness of the stainless steel, which was much greater, Fig. 1. The surface roughness of the coverslip was $R_a = 2.8$ nm $R_{ms} = 3.5$ nm, the tin oxide surface had a roughness of $R_a = 4.9$ nm, $R_{ms} = 6.3$ nm, while the stainless steel had a $R_a = 39.5$ nm and $R_{ms} = 52.4$ nm.

3.3. Cell activity

Cell metabolic activity as measured by the Almar Blue assay, Fig. 2. Cell activity is similar on all samples (one way ANOVA, $p = 0.256$ and $f = 1.722$). This shows that tin oxide shows no more cytotoxicity than stainless steel or glass.

3.4. Total DNA

Total DNA was measured using Hoechst 33258, Fig. 3. This indicated the number of cells on each sample. Again there was no significant difference between the

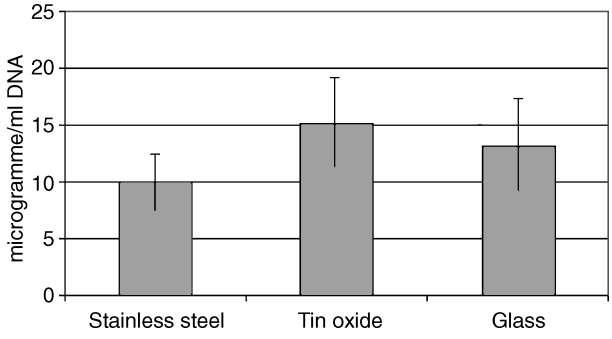

Figure 3 Graph of the μg of DNA per ml of cell extract. No significant difference between samples, one way ANOVA ($f = 0.804$, $p = 0.49$).

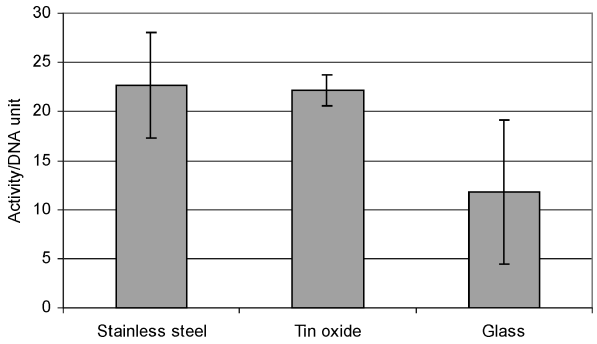

Figure 4 Graph of activity per DNA unit for each substrate. This was obtained by dividing the activity by the DNA value for each replicant. One way ANOVA shows that there is no significant difference between samples.

samples when measured using a one way ANOVA ($f = 0.804$, $p = 0.49$).

3.5. Activity per DNA unit

The graph in Fig. 4 shows the activity per DNA unit and was obtained by dividing the activity by the DNA value for each replicant. There is no significant difference between the samples.

3.6. SEM images of the cells

Cells grew on all three samples. Coverage on the glass surface was not complete (Fig. 5(a)). Cells were

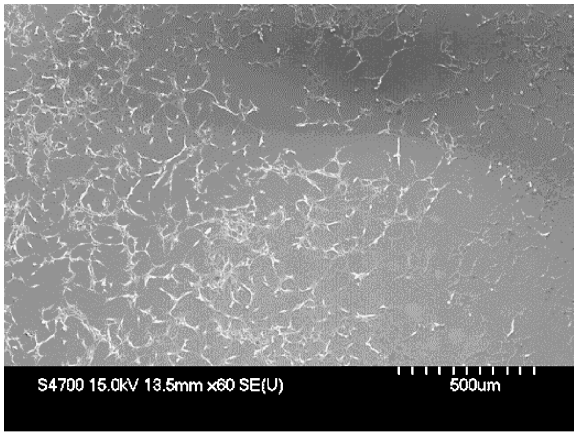

(a)

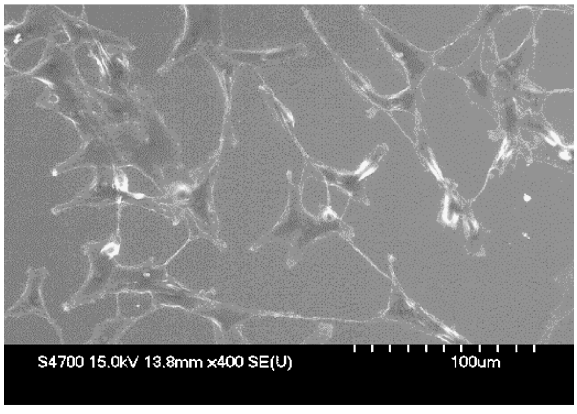

(b)

Figure 5 (a) Low magnification SEM image of cells growing on the glass substrate. (b) High magnification image of the cells on glass. The cells appear elongated on the surface, but there is incomplete coverage.

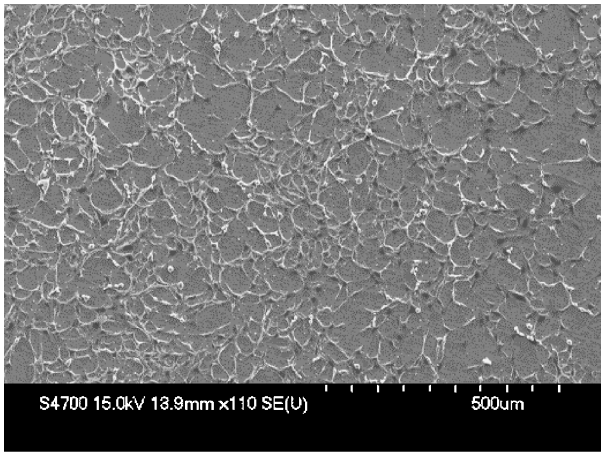

(a)

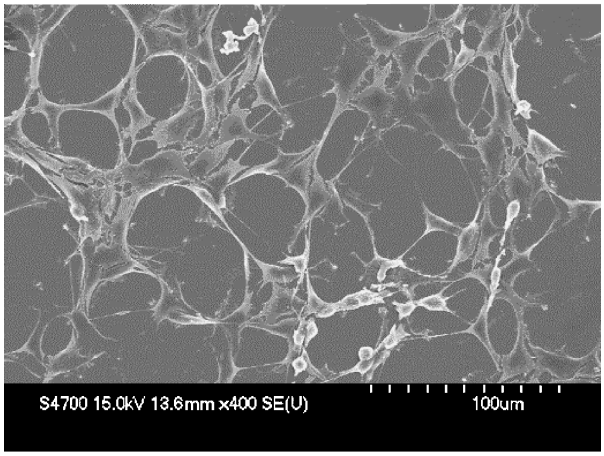

(b)

Figure 6 (a) Low magnification of cells growth on stainless steel. (b) High magnification image of cells on stainless steel. The filopodia are very extensive on the steel samples, coverage is incomplete.

well spread and elongated with long processes visible (Fig. 5(b)). Similarly, coverage was not complete on the stainless steel (Fig. 6(a)) although there was extensive cell coverage with cells forming an interconnecting network. Morphologically cells appeared as elongated on the glass sample but there were also numerous flattened cells surrounded by filopodia (Fig. 6(b)). In contrast the cells on the tin oxide surface showed extensive coverage with multilayered areas (Fig. 7(a)). Although occasional elongate or rounded cells (Fig. 7(b)) were visible the majority of the cells were flattened with numerous filopodia.

3.7. Circularity

The circularity (Fig. 8) describes the cell spreading on the surfaces of the samples. The stainless steel did not have full coverage and the cells appeared elongated. There was also incomplete coverage on the glass but the cells were well spread on the sample. There was complete coverage on the tin oxide surface with some evidence of multi-layer formation.

4. Discussion

As there is no significant difference between the activity per DNA unit of the samples, it can be inferred that

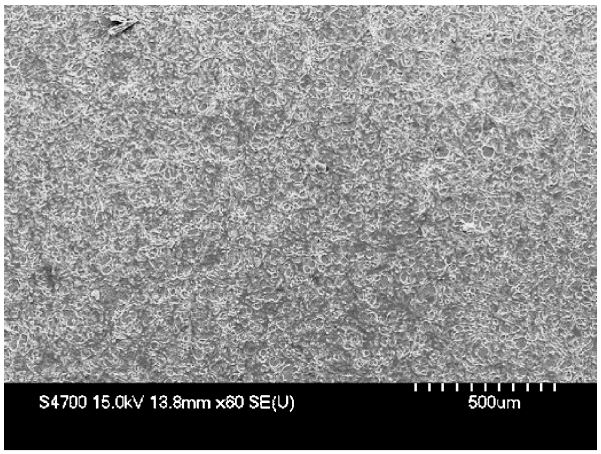

(a)

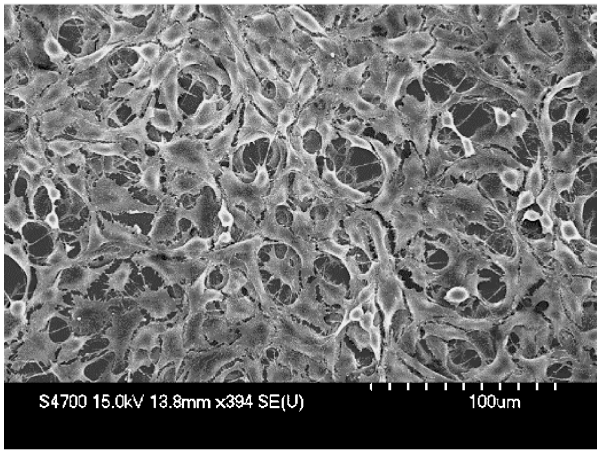

(b)

Figure 7 (a) Low magnification image of cells grown on tin oxide surface. (b) High magnification image. The images would seem to indicate that the cells are more numerous on the tin oxide surface than on the other two surfaces. There is complete coverage of the surface with cells and there is evidence of multi-layers.

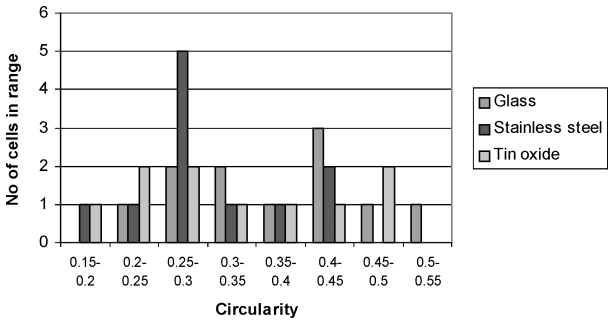

Figure 8 Graph of number of cells versus circularity. A circularity of 1 signifies a perfect circle, whereas a circularity of 0 indicates an elongated polygon. The significant peak between 0.25–0.3 for stainless steel indicates that the cells tend towards an elongated polygon, this is likely to be due to the elongation of the cells on the surface. The biggest peak for the glass shows that more cells were more rounded on this substrate. Cells on tin oxide were mostly well spread. There were a number of cells that were more rounded. This graph reflects the SEM images in Figs. 5–7.

the cells are equally active on each material. From this it may be inferred that the tin oxide coating does not stimulate any specific biological activity in 3T3 fibroblasts.

Cell responses to surfaces are dominated by two broad categories: chemistry and topography. Measurements of surface roughness will describe the topography. The tin oxide coating has a low R_a value. The limit of fibroblast responses to topography has been reported to be ~10 nm [30]. Therefore in the case of tin oxide, topography is unlikely to be the dominating factor. However, contact angle measurements have revealed that the tin oxide surface is highly wettable, i.e., hydrophilic. Although the specific influence of surface hydrophilicity on cell adhesion is still somewhat controversial [31], numerous studies have indicated that hydrophilic surfaces are particularly suitable for supporting cell adhesion. Cell spreading on the materials showed that cells were particularly well spread on the tin oxide surface. The graph of circularity (Fig. 8) shows that all the cells had a biphasic distribution of morphology. This would be logical based on the assumption that a population of viable cells would become rounded as they entered the cell cycle. Therefore cell attachment can be assessed by looking at the balance between rounded and spread cells. In the case of glass the largest peak is at 0.4–.0.45 with smaller peaks at 0.25–0.3, which indicates that the largest population of cells has a bias towards a rounded morphology. In contrast, stainless steel has the largest peak between 0.25–0.3 reflecting the more elongated morphology of the cells. It is clear therefore that the tin oxide coating supports cell growth and attachment at least as successfully as commercial stainless steel. However, on the stainless steel the tendency of the hydrophobic surface to prevent cell spreading has been offset by the surface roughness. This means that the surface wettability of the tin oxide and glass are the dominating property, while both the surface wettability and topography of the stainless steel contribute to the final cell response. Tin oxide has a peak between 0.45–0.5 and two further peaks between 0.2–0.3, this reflect the balance between the well spread cells seen on the SEM micrographs and the rounded morphology which may reflect cell proliferation.

References

1. R. HUBLER, *Surf. Coat. Techn.* **116–119** (1999) 1116.
2. R. HUBLER, A. COZZA, T. L. MARCONDES, R. B. SOUZA and F.F. FIORI, *ibid.* **142–144** (2001) 1078.
3. B. P. MCNAMARA, H. MURPHY and M. M. MORSHED, *Diam. Rel. Mater.* **10** (2001) 1098.
4. P. AEBISCHER, M. B. GODDARD, H. F. SASKEN, T. J. HUNTER and P. M. GALLETTI, *Biomaterials* **9** (1988) 80.
5. M. J. MUEHLBAUER, E. J. GUILBEAU, B. C. TOWE, and T. A. BRANDON, *Biosens. Bioelectr.* **5** (1990) 1.
6. F. HOLLSTEIN and P. LOUDA, *Surf. Coat. Techn.* **120–121** (1999) 627.
7. A. M. EKTESSABI, *Nucl. Instr. Meth. Phys. Res.* B **127/128** (1997).
8. A. M. EKTESSABI and H. KIMURA, *Thin Solid Films* **270** (1995) 335.
9. J. L. BUCHANAN and C. MCKOWN, *J. Non-Cryst. Solids* **218** (1997) 179.
10. J. DONG and H. D. GAFNEY, *ibid.* **203** (1996) 329.
11. R. GORDON, *ibid.* **218** (1997) 81.
12. R. J. MCCURDY, *Thin Solid Films* **351** (1999) 66.
13. G. DE, A. LICCIULLI, C. MASSARO, A. QUIRINI, R. RELLA, P. SICILIANO and L. VASANELLI, *Sens. Actuat.* B **55** (1999) 134.
14. M. A. EL KHAKANI, R. DOLBEC, A. M. SERVENTI, M. C. HORRILLO, M. TRUDEAU, R. G. SAINT-JACQUES, D. G. RICKERBY and I. SAYAGO, *ibid.* B **77** (2001) 383.

15. J. H. LUCAS, J. B. KIRKPATRICK and G. W. GROSS, *J Neur. Meth.* **14** (1985) 211.
16. E. TOMAI, H. L. BROWNELL, T. V. TUFESCU, K. REID, B. G. CAMPLING and L. RAPTIS, *Lung Cancer* **23** (1999) 223.
17. E. TOMAI, S. KLEIN, K. FIRTH and L. RAPTIS, *Prep. Biochem. Biotechn.* **30** (2000) 313.
18. G. W. GROSS, B. K. RHOADES, D. L. REUST and F. U. SCHWALM, *J. Neurosci. Meth.* **50** (1993) 131.
19. J. P. ESPINOS, A. FERNANDEZ, A. CABALLERO, V. M. JIMENEZ, J. C. SANCHEZLOPEZ, L. CONTRERAS, D. LEINEN and A. R. GONZALEZ-ELIPE, *Chem. Vap. Depoait.* **3** (1997) 219.
20. V. M. JIMENEZ, J. P. ESPINOS, A. CABALLERO, L. CONTRERAS, A. FERNANDEZ, A. JUSTO and A. R. GONZALEZ-ELIPE, *Thin Solid Films* **353** (1999) 113.
21. S. C. RAY, M. K. KARANJAI and D. DASGUPTA, *ibid.* **307** (1997) 221.
22. J. SZANYI, *Appl. Surf. Sci.* **185** (2002) 161.
23. I. A. KARAPATHITSKI, K. A. MIT, D. M. MUKHAMEDSHINA and N. B. BEISENKHANOV, *Surf. Coat. Techn.* **151/152** (2002) 76.
24. P. V. MCCRORY, E. C. COMBE and V. PIDDOCK, *Dent. Mater.* **14** (1998) 72.
25. C. COBIANU, C. SAVANIU, O. BUIU, D. DASCALU, M. ZAHARESCU, C. PARLOG, A. VAN DEN BERG and B. PECZ, *Sens. Actuat.* B **43** (1997) 114.
26. S. S. PARK, H. ZHENG and J. D. MACKENZIE, *Mater. Lett.* **22** (1995) 175.
27. M. V. LANCASTER and R. D. FIELDS, U.S. Patent no. 5,501,959 (1996).
28. R. RAGO, J. MITCHEN and G. WILDING, *Analyt. Biochem.* **191** (1990) 31.
29. B. D. RATNER, A. S. HOFFMAN, F. J. SCHOEN and J. E. LEMONS, in "Biomaterials Science: An Introduction to Materials in Medicine," 1996.
30. M. J. DALBY, M. O. RIEHLE, H. JOHNSTONE, S. AFFROSSMAN and A. S. G. CURTIS, *Cell. Biol. Intern.* **28** (2004) 229.
31. E. A. VOGLER, *Adv. Coll. Interf. Sci.* **74** (1998) 69.

Received 26 January
and accepted 19 July 2004